

# Cosmological parameter analyses using transversal BAO data

Rafael C. Nunes,<sup>1\*</sup> Santosh K. Yadav,<sup>2†</sup> J. F. Jesus,<sup>3,4‡</sup> Armando Bernui<sup>5§</sup>

<sup>1</sup>*Divisão de Astrofísica, Instituto Nacional de Pesquisas Espaciais, Avenida dos Astronautas 1758, São José dos Campos, 12227-010, SP, Brazil*

<sup>2</sup>*Department of Mathematics, BITS Pilani, Pilani Campus, Rajasthan-333031, India*

<sup>3</sup>*UNESP - Câmpus Experimental de Itapeva, Itapeva, SP, Brazil*

<sup>4</sup>*UNESP - Faculdade de Engenharia de Guaratinguetá, Guaratinguetá, SP, Brazil*

<sup>5</sup>*Observatório Nacional, Rua General José Cristino 77, São Cristóvão, 20921-400, Rio de Janeiro, RJ, Brazil*

Accepted XXX. Received YYY; in original form ZZZ

## ABSTRACT

We investigate observational constraints on cosmological parameters combining 15 measurements of the transversal BAO scale (obtained free of any fiducial cosmology) with Planck-CMB data to explore the parametric space of some cosmological models. We investigate how much Planck + transversal BAO data can constraint the minimum  $\Lambda$ CDM model, and extensions, including neutrinos mass scale  $M_\nu$ , and the possibility for a dynamical dark energy (DE) scenario. Assuming the  $\Lambda$ CDM cosmology, we find  $H_0 = 69.23 \pm 0.50 \text{ km s}^{-1} \text{ Mpc}^{-1}$ ,  $M_\nu < 0.11 \text{ eV}$  and  $r_{\text{drag}} = 147.59 \pm 0.26 \text{ Mpc}$  (the sound horizon at drag epoch) from Planck + transversal BAO data. When assuming a dynamical DE cosmology, we find that the inclusion of the BAO data can indeed break the degeneracy of the DE free parameters, improving the constraints on the full parameter space significantly. We note that the model is compatible with local measurements of  $H_0$  and there is no tension on  $H_0$  estimates in this dynamical DE context. Also, we discuss constraints and consequences from a joint analysis with the local  $H_0$  measurement from SH0ES. Finally, we perform a model-independent analysis for the deceleration parameter,  $q(z)$ , using only information from transversal BAO data.

**Key words:** Cosmological parameters – Dark energy

## 1 INTRODUCTION

Nowadays are stimulating for cosmology, with a plethora of dark energy models competing to describe the current high-quality cosmological observations (York et al. 2000; Ade et al. 2011). The combination of data from cosmological probes like standard candles, from type Ia supernovae data (Suzuki et al. 2012), standard rulers, from Baryon Acoustic Oscillations (BAO) data (Eisenstein et al. 2005; Aubourg et al. 2015; Ata et al. 2018), together with measurements of the cosmic microwave background (CMB) radiation (Hinshaw et al. 2013; Aghanim et al. 2018a) have produced precise parameters constraints of the concordance cosmological model, the spatially flat  $\Lambda$ CDM (Aghanim et al. 2018a; Shadab et al. 2017; Abbott et al. 2018), strongly restricting alternative scenarios (see, e.g., Ishak (2019); Nunes et al. (2017); D’Agostino & Nunes (2019); Capozziello et al. (2019); Yang et al. (2020); Vagnozzi et al. (2020); Di Valentino et al. (2020a); Anagnostopoulos et al. (2019); Lindner et al. (2020); Nesseris et al. (2019)).

To investigate cosmological models or parameters using observational data one usually performs a likelihood approach, which is done under basic assumptions. At the end, some hypothesis can be changed and the possible dependence of the results on such modification is studied. This is the case of the analyses of the CMB temperature fluctuations measurements, based on a power-law spectrum of adiabatic scalar perturbations, done by the Planck collaboration using a combination of temperature, polarization, and lensing CMB data. They found (Aghanim et al. 2018a) that the best-fit values of the spatially flat six parameter (i.e.,  $\Omega_b h^2$ ,  $\Omega_c h^2$ ,  $\theta_*$ ,  $\tau$ ,  $A_s$ ,  $n_s$ )  $\Lambda$ CDM model (here termed *minimum*  $\Lambda$ CDM) provides a good consistency with the data, with no indications for a preference on extensions of this basic set of parameters and hypotheses. Assuming this *minimum*  $\Lambda$ CDM cosmology, the Planck collaboration also found derived model-dependent parameters:  $H_0$ ,  $\Omega_m$ , and  $\sigma_8$  (Aghanim et al. 2018a). Additionally, combining CMB data with BAO measurements, they found (Aghanim et al. 2018a) that the neutrino mass is tightly constrained to  $M_\nu < 0.12 \text{ eV}$ , and that the effective extra relativistic degrees of freedom agrees with the prediction of the Standard Model  $N_{\text{eff}} = 3.046$ .

One cannot expect that the whole parameter space of the model will be well-behaved when describing the set of distinct cosmological probes used in several combined analysis.

\* E-mail: rafadcunes@gmail.com

† E-mail: sky91bbaulko@gmail.com

‡ E-mail: jf.jesus@unesp.br

§ E-mail: bernui@on.br

This is the case with the CMB lensing amplitude and the parameters related to, in fact, it was reported that the CMB spectra prefer higher lensing amplitudes than predicted in the *minimum*  $\Lambda$ CDM at over  $2\sigma$  [Aghanim et al. \(2018a\)](#). Another recognized tension is that one reported for the Hubble parameter  $H_0$ : while local SNIa observations measure  $H_0 = 74.03 \pm 1.42$  ([Riess et al. 2019](#)), the Planck collaboration report  $H_0 = 67.4 \pm 0.5 \text{ km s}^{-1} \text{ Mpc}^{-1}$  [Aghanim et al. \(2018a\)](#). And the question is how much dependent on model hypotheses are these results ([Sutherland 2012](#); [Heavens et al. 2014](#)) or do they reflect just measurements with underestimated systematics [Shanks et al. \(2019\)](#). For examples, of how systematics can influence data analyses see, e.g., [Bernui et al. \(2006, 2007, 2008\)](#); [Bengaly et al. \(2017\)](#); [Novaes et al. \(2014, 2015\)](#); [Marques et al. \(2018\)](#).

Current data analyses combine diverse cosmological probes to break degeneracy between cosmological parameters using, for instance, the data from Type IA supernova data or from Baryon Acoustic Oscillations (BAO). Regarding the use of the BAO data, an interesting issue refers to a possible bias in the standard BAO analysis due to the assumption of a fiducial cosmological model needed to calculate the fiducial comoving-coordinates, however, recent studies conclude that such assumption does not introduce any bias (see, e.g., [Aubourg et al. \(2015\)](#); [Vargas-Magaña et al. \(2018\)](#); [Carter et al. \(2020\)](#)). From the other side, the transversal BAO analysis does not need to assume a fiducial cosmology, and was also used for clustering analysis (see, e.g., [Sánchez et al. \(2011\)](#); [Carnero et al. \(2012\)](#); [Carvalho et al. \(2016\)](#)), although the precision of the angular BAO scale measurements with this methodology is not competitive with the standard one. Nevertheless, transversal BAO analyses complement standard BAO analyses and are interesting because: (a) transversal BAO studies, as described by [Sánchez et al. \(2011\)](#); [Carnero et al. \(2012\)](#) are weakly dependent on the assumption of a cosmological model, this allows a comparison with the results obtained with the standard BAO approach (comparisons are welcome in natural sciences, just as a validation or confirmation of results obtained by a different team using a distinct methodology); (b) since the transversal BAO only data needs angular distances between pairs to calculate the 2-point angular correlation function, these analysis (and their results) are independent of the 3D curvature parameter,  $\Omega_k$ , while in the standard BAO analysis this parameter has to be assumed (notice that the curvature parameter is being subject of a recent controversy [Di Valentino et al. \(2019a, 2020b\)](#)). (c) the methodology described by [Sánchez et al. \(2011\)](#) is a simple approach that lets to study the evolution of the Universe if one performs a tomographic study analyzing data in contiguous thin redshift shells, which are disjoint and separate in more than the uncertainties of the redshift measurements, this avoids the correlation between shells turning the measurements of  $D_A(z)/r_{\text{drag}}$  at several redshifts statistically independent. See [Salazar-Albornoz et al. \(2017\)](#); [Loureiro et al. \(2019\)](#); [Anselmi et al. \(2019\)](#); [O'Dwyer et al. \(2019\)](#); [Anselmi et al. \(2018\)](#); [Camarena & Marra \(2019\)](#); [Marra & Isidro \(2019\)](#) for others recent discussions on the cosmological constraints investigations under the perspective of the BAO measurements.

This work is organized as follows. In the next section, we provide an overview of contemporary cosmological parameters analyses, while in section 3 we present our data set and

the statistical methodology adopted. In section 4 we present the results and the related discussion of our analyses. In section 5 we perform a model-independent analysis on the  $q(z)$  function from the transversal BAO data and, in section 6, we summarize the findings of our analyses and express future perspectives.

## 2 COSMOLOGICAL PARAMETER ANALYSES

According to the above concerns, we perform cosmological parameter analyses combining CMB data with a set of 15 measurements of the transversal BAO scale measurements, obtained according to the model-independent approach of [Sánchez et al. \(2011\)](#), to explore via Monte Carlo Markov chains the parametric space of some cosmological models. Moreover, the literature shows the efforts to measure the sound horizon  $r_{\text{drag}}$  in a weakly model-dependent approach (see, e.g., [Sutherland \(2012\)](#); [Heavens et al. \(2014\)](#)). Following this objective, we shall combine data from Planck 2018 CMB data together with BAO, but using only the above mentioned 15 measurements of transversal BAO data  $D_A(z; r_{\text{drag}})$ . Complementing these analyses, we add the local Hubble parameter measurement ([Riess et al. 2019](#)) as a prior allowing a still more precise determination of  $r_{\text{drag}}$  at low redshift, in specific cases where the  $H_0$  tension is not present.

On the other hand, the neutrinos play a crucial role in the dynamics of our Universe, by inferring direct changes in the clustering of structures and, consequently, in the determination of cosmological parameters (see an incomplete list of works that investigates neutrino features ([Lesgourgues & Pastor 2006](#); [Lattanzi & Gerbino 2018](#); [Giusarma et al. 2016](#); [Nunes & Bonilla 2018b](#); [Marques et al. 2019](#); [Vagnozzi et al. 2017](#); [Di Valentino et al. 2019b](#)) and references therein). The standard parameters that characterize these effects are the effective number of neutrino species  $N_{\text{eff}}$  and the total neutrino mass scale  $M_\nu$ . We refer to ([Aghanim et al. 2018a](#); [Di Valentino et al. 2019b](#)) for recent constraints on these parameters. In principle, both quantities  $N_{\text{eff}}$  and  $M_\nu$  are model dependent, and hence, different cosmological scenarios may bound these parameters in different ways. In our analysis, we consider that recent measurements of the transversal BAO signature can help to a better constraint of the neutrinos mass scale. It will be the first time that such data sets will be used to investigate these properties of neutrinos.

According to this plan, we combine for the first time a compilation of these angular BAO measurements, with the following aims:

(i) To perform combined analyses that explores the parameters space of some dark energy (DE) models and, additionally, to obtain a precise estimate of  $r_{\text{drag}}$  from each model. This is due to the fact that the inclusion of transversal BAO data will improve estimates on matter density and Hubble constant, which, in return, will also improve the bounds on  $r_{\text{drag}}$ .

(ii) To derive new bounds on the neutrino mass scale  $M_\nu$  within  $\Lambda$ CDM and extended models, considering the possibility for some dynamical dark energy scenarios, robustly

using transversal BAO data.

(iii) An independent model analysis to reconstruct the deceleration parameter  $q(z)$  from our compilation of transverse BAO data.

The cosmological model analyses mentioned above in the points (i) and (ii) encompass two scenarios: the current concordance model, i.e., the spatially flat  $\Lambda$ CDM, and the simplest natural extension to the  $\Lambda$ CDM model, that is, a dynamical DE model,  $w_0$ - $w_a$ CDM considering the Chevallier-Polarski-Linder (CPL) parameterization (Chevallier & Polarski 2001; Linder 2003), where the EoS is characterized by  $w(a) = w_0 + w_a(1 - a)$ , where  $a$  is the scale factor in a Friedmann-Robertson-Walker cosmology.

Our main results show that the joint analyses of CMB data and transversal BAO measurements improves the parameter constraints, also in the case where we include the neutrino mass as an extra-parameter. Moreover, we also recover the best-fit values of the *minimum*  $\Lambda$ CDM model (Aghanim et al. 2018a), concerning the main baseline and derived cosmological parameters, with improved values when including BAO data.

### 3 DATA AND METHODOLOGY

In what follows, we describe the observational data sets used in this work.

**BAO:** First, we describe the set of 15 transversal BAO measurements,  $\theta_{\text{BAO}}(z)$ , obtained without assuming a fiducial cosmological model (Sánchez et al. 2011; Carnero et al. 2012). In fact, in a thin redshift bin with suitable number density of cosmic tracers –like quasars or galaxies–, one can perform the 2-point angular correlation function between pairs to find and measure the BAO angular scale  $\theta_{\text{BAO}}(z)$ , at that redshift (see, e.g., (Carvalho et al. 2016) and refs. therein). A BAO angular scale measurement gives the angular diameter distance  $D_A$  at the redshift  $z$

$$D_A(z; r_{\text{drag}}) = \frac{r_{\text{drag}}}{(1+z)\theta_{\text{BAO}}(z)}, \quad (1)$$

provided that one has a robust estimate of  $r_{\text{drag}}$ , the comoving sound horizon at the baryon drag epoch.

Our set of 15 transversal BAO measurements (Carvalho et al. 2016; Alcaniz et al. 2017; Carvalho et al. 2020; de Carvalho et al. 2018, 2020), were obtained using public data releases (DR) of the Sloan Digital Sky Survey (SDSS), namely: DR7, DR10, DR11, DR12, DR12Q (quasars) (York et al. 2000). These data set is displayed in Table 1. It is important to notice that, due to the cosmological-independent methodology used to perform these transversal BAO measurements their errors are larger than the errors obtained using a fiducial cosmology approach. The reason for this fact is that, while in the former methodology the error is given by the measure of how large is the BAO bump, in the later approach the model-dependent best-fit of the BAO signal quantifies a smaller error. Typically, in the former methodology the error can be of the order of  $\sim 10\%$ , but in some cases it can arrive to 18%, and in the later approach it is of the order of few percent (Sánchez et al. 2011).

$z$	$\theta_{\text{BAO}}$ [deg]	$\sigma_{\text{BAO}}$ [deg]	ref.
0.11	19.8	3.26	de Carvalho et al. (2020)
0.235	9.06	0.23	Alcaniz et al. (2017)
0.365	6.33	0.22	Alcaniz et al. (2017)
0.45	4.77	0.17	Carvalho et al. (2016)
0.47	5.02	0.25	Carvalho et al. (2016)
0.49	4.99	0.21	Carvalho et al. (2016)
0.51	4.81	0.17	Carvalho et al. (2016)
0.53	4.29	0.30	Carvalho et al. (2016)
0.55	4.25	0.25	Carvalho et al. (2016)
0.57	4.59	0.36	Carvalho et al. (2020)
0.59	4.39	0.33	Carvalho et al. (2020)
0.61	3.85	0.31	Carvalho et al. (2020)
0.63	3.90	0.43	Carvalho et al. (2020)
0.65	3.55	0.16	Carvalho et al. (2020)
2.225	1.77	0.31	de Carvalho et al. (2018)

**Table 1.** A compilation of angular BAO measurements from luminous red galaxies, blue galaxies, and quasars catalogs, from diverse releases of the Sloan Digital Sky Survey, all of them obtained following the approach of Sánchez et al. (2011).

**CMB:** To break the degeneracy, when considering the full parametric space of the models under study in this work, we shall combine this BAO data set (see Table 1) together with the CMB data from the final release of the Planck collaboration (2018), including the likelihood TT+TE+EE+lowE+lensing (Aghanim et al. 2018a,b, 2019). Here we just refer this data set as Planck.

**R19:** In some analyses, we shall consider the recently measured new local value of the Hubble constant by the Hubble Space Telescope (HST):  $H_0 = 74.03 \pm 1.42 \text{ km s}^{-1} \text{ Mpc}^{-1}$  as reported in (Riess et al. 2019). This value of the Hubble constant is in tension, at  $4.4\sigma$ , with the Planck 2018 cosmological parameters calculation within the minimum  $\Lambda$ CDM model Aghanim et al. (2018a). We refer to this datum as R19.

Regarding the theoretical framework, let us consider two scenarios in our analyses. The first scenario, termed  $\Lambda$ CDM +  $M_\nu$ , described from the baseline

$$\mathcal{P} \equiv \left\{ \omega_b, \omega_{\text{CDM}}, 100\theta_*, \tau_{\text{reio}}, n_s, \log[10^{10} A_s], M_\nu \right\}, \quad (2)$$

where the first six parameters corresponds to the minimum  $\Lambda$ CDM model: the baryon and the cold dark matter energy densities  $\omega_b$  and  $\omega_{\text{cdm}}$ , the ratio between the sound horizon and the angular diameter distance at decoupling  $100\theta_*$ , the reionization optical depth  $\tau_{\text{reio}}$ , and the spectral index and the amplitude of the scalar primordial power spectrum  $n_s$  and  $A_s$ , respectively.

With respect to the neutrino properties, we impose a prior of  $M_\nu > 0$ , ignoring a possible lower limit from the neutrino oscillations experiments and assuming fixed three neutrinos species, that is,  $N_{\text{eff}} = 3.046$ . For the purposes of obtaining bounds on neutrino mass from the cosmological data, the prior  $M_\nu > 0$  is adequate.

The second scenario, we will consider a dynamical DE model, where the EoS is given in terms of the CPL parametrization. Let us call this model by  $w_0$ - $w_a$ CDM model.

In this case, the parametric space is written as

$$\mathcal{P} \equiv \left\{ \omega_b, \omega_{\text{CDM}}, 100\theta_*, \tau_{\text{reio}}, n_s, \log[10^{10} A_s], w_0, w_a, M_\nu \right\}, \quad (3)$$

where  $w_0$  and  $w_a$ , are free parameters that characterize the dynamics of the EoS, where for  $w_0 = -1$  and  $w_a = 0$ , we recovered the  $\Lambda$ CDM model.

We use the publicly available CLASS (Blas et al. 2011) and MontePython (Audren et al. 2013) codes to analyze the free parameters of the models defined above. We used Metropolis Hastings algorithm with uniform priors on the full baseline parameters to obtain correlated Markov Chain Monte Carlo samples. We have ensured the convergence of the chains for all parameters according to the Gelman-Rubin criterium. During the statistical analyses, we consider the flat priors on all parameters, where the common baseline parameters in all scenarios is:  $100\omega_b \in [0.8, 2.4]$ ,  $\omega_{\text{cdm}} \in [0.01, 0.99]$ ,  $100\theta_* \in [0.5, 2]$ ,  $\tau_{\text{reio}} \in [0.01, 0.8]$ ,  $\log_{10}(10^{10} A_s) \in [2, 4]$ ,  $n_s \in [0.9, 1.1]$ ,  $w_0 \in [-3, 0]$ ,  $w_a \in [-3, 3]$ , and  $M_\nu \in [0, 1]$ . The  $\Lambda$ CDM model is obtained by fixing  $w_0 = -1$  and  $w_a = 0$ . We assume a spatially flat Universe in all analyzes performed in this work. As usual, the parameters  $H_0, \sigma_8, r_s$ , and  $\Omega_m$  are derived parameters. In what follows we discuss our results.

## 4 COMBINED ANALYSES OF CMB PLUS TRANSVERSAL BAO DATA

Throughout this section we will present our main results.

### 4.0.1 $\Lambda$ CDM scenario

For the  $\Lambda$ CDM +  $M_\nu$  model, we summarize the main observational results in Table 2. For comparison, we also show analyses without and with neutrinos.

Assuming the  $\Lambda$ CDM scenario, we notice that adding the BAO data in a combined analysis with Planck, the constraints on the parameters that are most sensitive to geometrical tests, like  $\Omega_m$  and  $H_0$ , are significantly improved. In fact, from Planck + transversal BAO analysis, the constraint on  $H_0$  and  $\Omega_m$  is significantly deviated to a higher and lower fit value, respectively, when compared with the analysis from Planck data only. However, the difference on these parameters between the analyses Planck + transversal BAO versus Planck data only, as well as for the other parameters in the baseline are compatible with each other at 68% CL. Thus, we can note compatibility between Planck and transversal BAO data, including the fact that the addition of BAO data helps to break possible degeneracy in the parameters space, is an excellent outcome of the current analyses.

From the Planck data only, we obtain  $H_0 = 67.39 \pm 0.56$  km s<sup>-1</sup> Mpc<sup>-1</sup>, while  $H_0 = 69.23 \pm 0.50$  km s<sup>-1</sup> Mpc<sup>-1</sup> from Planck + transversal BAO data, in both cases at 68% CL. The value obtained by the Planck team from CMB + BAO data<sup>1</sup> is  $H_0 = 67.77 \pm 0.42$ . It is well reported in the literature that there is a strong tension between the  $H_0$  estimates done by the Planck collaboration and local measurements as reported by Riess et al. Riess et al. (2019), i.e.,  $H_0 = 74.03 \pm 1.42$  km s<sup>-1</sup> Mpc<sup>-1</sup>. One can notice that

<sup>1</sup> See section 5.1 in Aghanim et al. (2018a) for details of the BAO data points used in the analyses done by the Planck collaboration.

the combined analyses done here, using Planck + transversal BAO data, minimally alleviate this tension, but a tension at more than  $3\sigma$  still remains. The difference on the  $H_0$  parameter between the Planck team constraints and our results is approximately  $\sim 1.4\sigma$ .

In the left panel of Figure 1, we show the confidence level contours in the parametric space  $r_{\text{drag}} - H_0$  from all our analyses using  $\Lambda$ CDM model. Some words are in due here regarding  $r_{\text{drag}}$ . This quantity is not directly measured by CMB data, its calculation depends on model hypotheses of early time physics, for this it is obtained in a model-dependent way in CMB analyses (Sutherland 2012; Heavens et al. 2014; Aghanim et al. 2018a). Both parameters,  $r_{\text{drag}}$  and  $H_0$ , provide an absolute scale for distance measurements at opposite ends of the observable universe,  $r_{\text{drag}}$  (early time) and  $H_0$  (late time). When measured with the same data, these parameters must agree with the values predicted by the standard cosmological model. Otherwise, significant deviations of these parameters with respect to the expected values would provide indications for some new physics beyond the standard model, or unaccounted systematic errors in the measurements. Planck team reported the value  $r_{\text{drag}} = 147.21 \pm 0.23$  from CMB + BAO at 68% CL in  $\Lambda$ CDM cosmology (Aghanim et al. 2018a). These estimates are not only compatible, but very similar to ours, in all analyzes (see Table 2). On the other hand, a model-independent reconstruction from the early-time physics shows that  $r_{\text{drag}} = 136.7 \pm 4.1$  (Bernal et al. 2016). As argued by Bernal et al. (2016), this strong tension in the  $r_{\text{drag}}$  measurement is entirely due to the tension in the  $H_0$  parameter, via the strong correlation between  $H_0$  and  $r_{\text{drag}}$  parameters. Considering a physics beyond the standard model, in ref. (Kumar et al. 2018) it is assumed a dark coupling between dark matter and photons, an approach that can reconcile the tension in both parameters,  $H_0$  and  $r_{\text{drag}}$ . Another proposal for some new physics in light the  $H_0$  and  $r_{\text{drag}}$  tension at early and/or late time modification in the standard cosmological model was also proposed in (Nunes 2018a; Kumar et al. 2019; Poulin et al. 2019; Di Valentino et al. 2020a; Vagnozzi 2019; Pan et al. 2019a,b; Yang et al. 2018).

In the right panel of Figure 1, we show the confidence level contours in the parametric plane  $\Omega_m - M_\nu$ , where we find  $M_\nu < 0.11$  eV at 95% CL from Planck + transversal BAO data. That boundary on the neutrino mass scale is practically the same as that one reported by the Planck team using Planck CMB + BAO, i.e.,  $M_\nu < 0.12$  eV. Some minimal displacement can be noted on the  $\Omega_m$  best fit value, but again, the constraints are fully compatible with each other at 68% CL. Thus, we conclude that the combination of the transversal BAO and CMB data can bound  $M_\nu$  with the same accuracy than other joint analyses reported in the literature.

### 4.0.2 $w_0$ - $w_a$ CDM scenario

In view of the capacity of the transversal BAO data to breaks the degeneracy on some cosmological parameters, let us study how these data could bound some dynamical effect of dark energy. In Table 3, we summarize the results of our statistical analyses from the perspective of the  $w_0$ - $w_a$ CDM model. As already known, assuming a  $w_0$ - $w_a$ CDM model, the con-



Parameter	Planck		Planck + BAO	
	$\Lambda$ CDM	$\Lambda$ CDM + $M_\nu$	$\Lambda$ CDM	$\Lambda$ CDM + $M_\nu$
$10^2\omega_b$	$2.240^{+0.015+0.031}_{-0.015-0.029}$	$2.233^{+0.015+0.029}_{-0.015-0.029}$	$2.260^{+0.014+0.028}_{-0.014-0.027}$	$2.258^{+0.015+0.027}_{-0.014-0.027}$
$\omega_{\text{CDM}}$	$0.1199^{+0.0012+0.0024}_{-0.0012-0.0024}$	$0.1206^{+0.0013+0.0025}_{-0.0013-0.0024}$	$0.1206^{+0.0013+0.0025}_{-0.0013-0.0024}$	$0.1172^{+0.0011+0.0021}_{-0.0011-0.0021}$
$100\theta_*$	$1.0419^{+0.0003+0.0006}_{-0.0003-0.0006}$	$1.0418^{+0.0003+0.0006}_{-0.0003-0.0006}$	$1.0421^{+0.0003+0.0005}_{-0.0003-0.0006}$	$1.0421^{+0.0003+0.0005}_{-0.0003-0.0006}$
$\ln 10^{10} A_s$	$3.044^{+0.014+0.027}_{-0.014-0.028}$	$3.048^{+0.015+0.030}_{-0.015-0.029}$	$3.055^{+0.016+0.031}_{-0.016-0.030}$	$3.061^{+0.016+0.031}_{-0.016-0.030}$
$n_s$	$0.965^{+0.004+0.008}_{-0.004-0.008}$	$0.963^{+0.004+0.008}_{-0.004-0.008}$	$0.971^{+0.004+0.008}_{-0.004-0.008}$	$0.971^{+0.004+0.008}_{-0.004-0.008}$
$\tau_{\text{reio}}$	$0.054^{+0.007+0.015}_{-0.007-0.014}$	$0.055^{+0.007+0.015}_{-0.008-0.014}$	$0.062^{+0.007+0.016}_{-0.008-0.015}$	$0.064^{+0.008+0.016}_{-0.008-0.016}$
$M_\nu$	--	< 0.34	--	< 0.11
$\Omega_m$	$0.308^{+0.007+0.015}_{-0.007-0.014}$	$0.326^{+0.009+0.025}_{-0.013-0.022}$	$0.292^{+0.006+0.012}_{-0.006-0.012}$	$0.299^{+0.006+0.014}_{-0.006-0.013}$
$H_0$	$67.39^{+0.56+1.10}_{-0.56-1.10}$	$66.59^{+0.96+1.60}_{-0.67-1.80}$	$69.23^{+0.50+1.00}_{-0.50-0.97}$	$68.58^{+0.54+1.00}_{-0.54-1.10}$
$\sigma_8$	$0.82^{+0.006+0.012}_{-0.006-0.012}$	$0.800^{+0.0150+0.022}_{-0.007-0.028}$	$0.819^{+0.006+0.013}_{-0.006-0.012}$	$0.807^{+0.006+0.013}_{-0.006-0.013}$
$r_{\text{drag}}$	$147.09^{+0.27+0.52}_{-0.27-0.51}$	$147.97^{+0.28+0.53}_{-0.28-0.56}$	$147.59^{+0.25+0.48}_{-0.25-0.48}$	$147.59^{+0.26+0.51}_{-0.26-0.52}$

**Table 2.** Constraints at 68% and 95% CL on free and some derived parameters under  $\Lambda$ CDM model baseline from the considered data combinations. The parameter  $H_0$  is measured in the units of km/s/Mpc,  $r_{\text{drag}}$  in Mpc, whereas  $M_\nu$  is in the units of eV.

Parameter	Planck		Planck + BAO	
	$w_0$ - $w_a$ CDM	$w_0$ - $w_a$ CDM + $M_\nu$	$w_0$ - $w_a$ CDM	$w_0$ - $w_a$ CDM + $M_\nu$
$10^2\omega_b$	$2.245^{+0.015+0.028}_{-0.015-0.028}$	$2.237^{+0.015+0.030}_{-0.015-0.029}$	$2.243^{+0.013+0.029}_{-0.015-0.026}$	$2.240^{+0.015+0.029}_{-0.015-0.029}$
$\omega_{\text{CDM}}$	$0.1192^{+0.0013+0.0028}_{-0.0013-0.0026}$	$0.1299^{+0.0013+0.0027}_{-0.0013-0.0025}$	$0.1192^{+0.0011+0.0022}_{-0.0011-0.0023}$	$0.1198^{+0.0012+0.0023}_{-0.0012-0.0023}$
$100\theta_*$	$1.0419^{+0.0003+0.0006}_{-0.0003-0.0006}$	$1.0419^{+0.0003+0.0006}_{-0.0003-0.0006}$	$1.0421^{+0.0003+0.0005}_{-0.0003-0.0005}$	$1.0421^{+0.0003+0.0005}_{-0.0003-0.0006}$
$\ln 10^{10} A_s$	$3.038^{+0.015+0.029}_{-0.015-0.030}$	$3.043^{+0.015+0.030}_{-0.015-0.030}$	$3.037^{+0.015+0.031}_{-0.015-0.029}$	$3.043^{+0.014+0.030}_{-0.014-0.027}$
$n_s$	$0.967^{+0.004+0.008}_{-0.004-0.008}$	$0.965^{+0.004+0.009}_{-0.004-0.009}$	$0.967^{+0.004+0.008}_{-0.004-0.008}$	$0.965^{+0.004+0.008}_{-0.004-0.008}$
$\tau_{\text{reio}}$	$0.052^{+0.007+0.014}_{-0.007-0.015}$	$0.054^{+0.007+0.015}_{-0.007-0.014}$	$0.052^{+0.008+0.015}_{-0.008-0.015}$	$0.054^{+0.007+0.016}_{-0.007-0.014}$
$w_0$	$-1.28^{+0.42+0.71}_{-0.68-0.72}$	$-1.51^{+0.56+0.62}_{-0.48-0.52}$	$-0.92^{+0.29+0.39}_{-0.14-0.52}$	$-1.04^{+0.30+0.42}_{-0.15-0.53}$
$w_a$	$-0.70^{+0.77+1.50}_{-1.30-1.30}$	$-0.58^{+0.86+1.30}_{-0.86-1.40}$	$-1.11^{+0.28+1.60}_{-0.86-0.94}$	$-1.11^{+0.28+1.60}_{-0.88-0.93}$
$M_\nu$	--	< 0.38	--	< 0.33
$\Omega_m$	$0.222^{+0.073+0.120}_{-0.073-0.120}$	$0.205^{+0.024+0.150}_{-0.081-0.092}$	$0.259^{+0.021+0.035}_{-0.017-0.040}$	$0.253^{+0.021+0.038}_{-0.018-0.040}$
$H_0$	$83.0^{+10.4+30.0}_{-20.0-20.0}$	$87.0^{+10.0+20.0}_{-20.0-20.0}$	$74.1^{+2.1+5.7}_{-3.3-5.1}$	$75.6^{+2.4+6.4}_{-3.5-5.8}$
$\sigma_8$	$0.940^{+0.120+0.200}_{-0.140-0.170}$	$0.956^{+0.120+0.160}_{-0.070-0.190}$	$0.875^{+0.022+0.049}_{-0.027-0.047}$	$0.875^{+0.021+0.055}_{-0.030-0.051}$
$r_{\text{drag}}$	$147.23^{+0.29+0.59}_{-0.29-0.59}$	$147.09^{+0.30+0.54}_{-0.27-0.58}$	$147.24^{+0.25+0.48}_{-0.25-0.48}$	$147.11^{+0.26+0.49}_{-0.26-0.52}$

**Table 3.** Constraints at 68% and 95% CL on free and some derived parameters under  $w_0$ - $w_a$ CDM model baseline from the considered data combinations. The parameter  $H_0$  is measured in the units of km/s/Mpc,  $r_{\text{drag}}$  in Mpc, whereas  $M_\nu$  is in the units of eV.

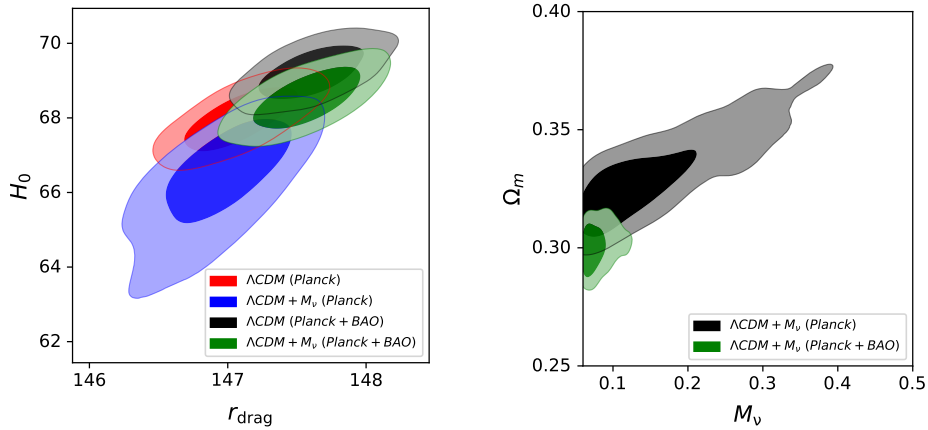


**Figure 1.** Results from the  $\Lambda$ CDM cosmology. Left panel: Constraints at 68% and 95% CL in the parametric space  $r_{\text{drag}} - H_0$  from Planck data only and Planck + transversal BAO, with and without the addition of neutrinos mass scale  $M_\nu$  as a free parameter. Right panel: Constraints in the plan  $\Omega_m - M_\nu$ , under perspectives of the scenario  $\Lambda$ CDM +  $M_\nu$ .

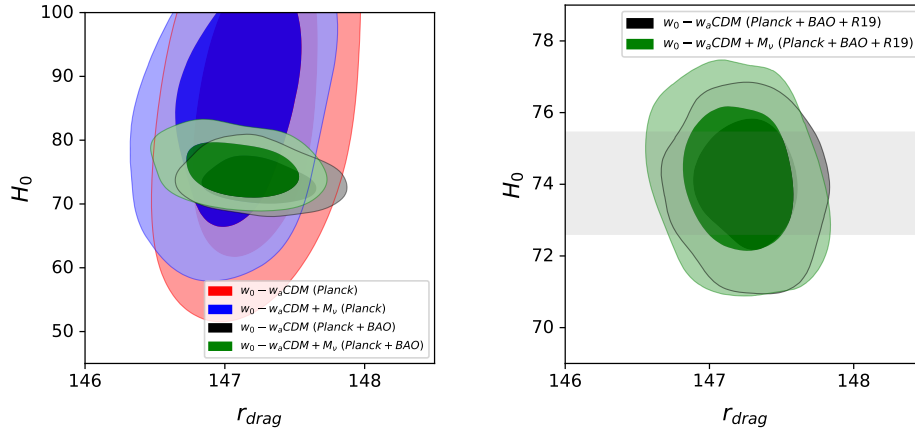


**Figure 2.** Left panel: The 68% CL and 95% CL regions in the plan  $r_{\text{drag}} - H_0$  inferring from  $w_0 - w_a$ CDM model using Planck data only and Planck + transversal BAO. Right panel: The same as left panel, but a joint analysis from Planck + transversal BAO + R19. The vertical light red band corresponds to measure  $H_0 = 74.03 \pm 1.42 \text{ km s}^{-1} \text{ Mpc}^{-1}$ .

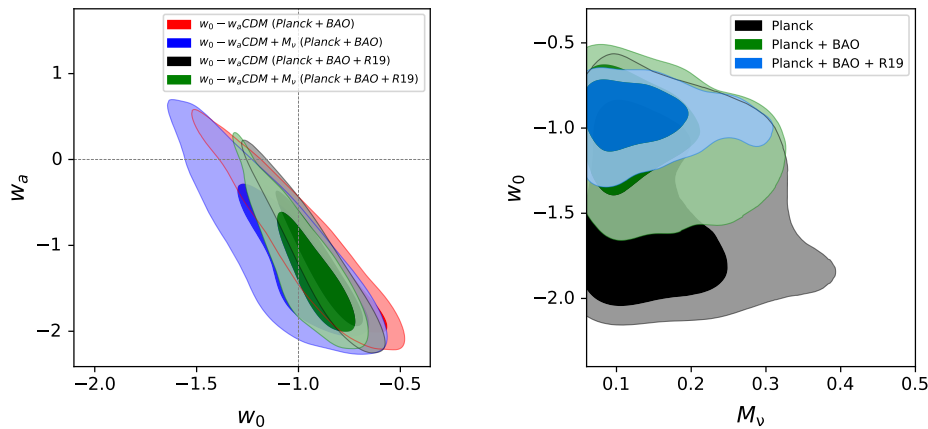


**Figure 3.** Left panel: Parametric space at 68% CL and 95% CL in the plan  $w_0 - w_a$  from the considered data combinations. Right panel: Confidence regions at 68% CL and 95% CL in the plan  $M_\nu - w_0$  from the  $w_0 - w_a$ CDM model in terms of the considered data combinations.

straints on  $H_0$  become degenerate in such way to obtain high  $H_0$  values enough to be compatible with local measurements.. We combine Planck data with transversal BAO data to break the degeneracy on the full baseline parameters of the model, finding  $H_0 = 74.1^{+2.1}_{-3.3} \text{ km s}^{-1} \text{ Mpc}^{-1}$  (without neutrinos) and  $H_0 = 75.6^{+2.4}_{-3.5} \text{ km s}^{-1} \text{ Mpc}^{-1}$  (including neutrinos), both at 68% CL. Thus, we can clearly notice that by adding transversal BAO data, the analysis significantly improves the bounds on  $H_0$  when compared to Planck data only. More specifically, it is obtained an improvement of  $\sim 24\%$  and  $\sim 32\%$  on  $H_0$  in the analysis without and with neutrinos, respectively. See  $H_0$  value from Planck data only in Table 3 for this same scenario. Additionally, these constraints are fully compatible with local estimate of  $H_0$  from HST. Thus, the current tension on  $H_0$  present in  $\Lambda$ CDM model, does not persist within this scenario, and the combination Planck + transversal BAO is not in tension with local measures. We conclude that dynamical models, like  $w_0 - w_a$ CDM, can solve the tension on the  $H_0$  parameter. In view of this, let us also consider the joint analysis Planck + transversal BAO + R19 data. These results are summarized in Table 4.

Figure 2 shows the parametric space in the plane  $r_{\text{drag}} -$

$H_0$ . On the left panel, we quantify the improvements due to the inclusion of the transversal BAO data. On the right panel, we have the joint analyses Planck + BAO + R19. With respect to the  $r_{\text{drag}}$  parameter, we do not notice any significant deviations as compared with the results predicted for the minimum  $\Lambda$ CDM model. Figure 3 on the left panel shows the constraints in the plane  $w_0 - w_a$  from Planck + BAO and Planck + BAO + R19 data combination. We can see that transversal BAO data set significantly improves the constraints on the EoS parameters, in comparison with Planck data only. We find an improvement of  $\sim 54\%$  and  $\sim 38\%$  on  $w_0$  and  $w_a$ , respectively, from the analysis without the presence of neutrinos. Instead, with neutrinos we find an improvement of  $\sim 67\%$  and  $\sim 39\%$  on  $w_0$  and  $w_a$ , respectively. We found no evidence for deviations of the minimum  $\Lambda$ CDM cosmology, even when including the R19 datum in the analysis. In the right panel of Figure 3 we show the relationship between  $w_0 - M_\nu$  and the effect on the confidence contour levels due to diverse combined data analyses. We observe that the bound on the neutrino mass scale is slightly decreased, while the constraints on the  $w_0$  parameter are more robust, significantly improving the restrictions when considering the joint analysis Planck + BAO

Parameter	Planck + BAO + R19	Planck + BAO + R19
	$w_0$ - $w_a$ CDM + $M_\nu$	$w_0$ - $w_a$ CDM
$10^2\omega_b$	$2.242^{+0.015+0.029}_{-0.015-0.030}$	$2.245^{+0.014+0.028}_{-0.014-0.027}$
$\omega_{\text{CDM}}$	$0.1194^{+0.0012+0.0024}_{-0.0012-0.0025}$	$0.1192^{+0.0011+0.0023}_{-0.0011-0.0022}$
$100\theta_*$	$1.04195^{+0.00030+0.00056}_{-0.00030-0.00058}$	$1.04193^{+0.00029+0.00058}_{-0.00029-0.00056}$
$\ln 10^{10} A_s$	$3.045^{+0.016+0.032}_{-0.016-0.030}$	$3.037^{+0.014+0.027}_{-0.014-0.028}$
$n_s$	$0.9658^{+0.0043+0.0086}_{-0.0043-0.0083}$	$0.9667^{+0.0041+0.0080}_{-0.0041-0.0084}$
$\tau_{\text{reio}}$	$0.0552^{+0.0081+0.017}_{-0.0081-0.015}$	$0.0520^{+0.0074+0.015}_{-0.0074-0.015}$
$w_0$	$-0.920^{+0.15+0.23}_{-0.095-0.27}$	$-0.89^{+0.17+0.25}_{-0.11-0.29}$
$w_a$	$-1.39^{+0.18+0.97}_{-0.59-0.64}$	$-1.23^{+0.30+1.0}_{-0.68-0.80}$
$M_\nu$	$< 0.31$	—
$\Omega_m$	$0.2602^{+0.0092+0.019}_{-0.0092-0.017}$	$0.2594^{+0.0087+0.017}_{-0.0087-0.017}$
$H_0$	$74.2^{+1.4+2.6}_{-1.4-2.6}$	$73.9^{+1.2+2.4}_{-1.2-2.4}$
$\sigma_8$	$0.864^{+0.015+0.030+}_{-0.015-0.029}$	$0.874^{+0.014+0.028}_{-0.014-0.027}$
$r_{\text{drag}}$	$147.18^{+0.27+0.52}_{-0.27-0.53}$	$147.23^{+0.25+0.50}_{-0.25-0.48}$

**Table 4.** Constraints at 68% and 95% CL on free and some derived parameters under  $w_0$ - $w_a$ CDM model baseline from the considered data combinations. The parameter  $H_0$  is measured in the units of km/s/Mpc,  $r_{\text{drag}}$  in Mpc, whereas  $M_\nu$  is in the units of eV

and Planck + BAO + R19. We found  $M_\nu < 0.38, 0.33, 0.31$  eV at 95% CL, from Planck, Planck + BAO, and Planck + BAO + R19 data sets, respectively. The final effect is that the presence of a dynamical dark energy component slightly extends the bound on  $M_\nu$ , as compared to  $\Lambda$ CDM model prediction. Effects of the neutrino mass scale on some dynamical dark energy models are also discussed in (Yang et al. 2017; Vagnozzi et al. 2018; Choudhury & Choubey 2018), but these studies consider other data sets. Our results represents a new update on  $M_\nu$  through the use of our recent transversal BAO data compilation.

The fact that  $w_0$ - $w_a$ CDM scenario can generate high  $H_0$  values, is due the feature that the scenario predict less dark matter today –in contrast, more dark energy– via the relation  $\Omega_m + \Omega_{DE} = 1$ , where  $\Omega_m = \Omega_b + \Omega_{DM}$ , in direct comparison with the  $\Lambda$ CDM best fit values. Notice that  $\Omega_b$  is fully compatible in all these scenarios. So, the change on  $\Omega_m$  estimates is due to dark matter density only, once the radiation (photons + neutrinos) contribution is negligible at  $z = 0$ . Because this scenario predicts more dark energy at late times, the universe expands faster than predicted in the  $\Lambda$ CDM cosmology, generating a larger  $H(z)$  and, at the same time, changing the slope of the Sachs-Wolfe plateau, that is, the late-time integrated Sachs-Wolfe effect (ISW), where the amplitude of the ISW effect will depend on the duration of the dark energy-dominated phase, which is basically managed by the ratio  $\Omega_{DM}/\Omega_{DE}$ . The  $H_0$  value from CMB data is inferred analyzing the first acoustic peak position, which depends on the angular scale  $\theta_* = d_s^*/D_A^*$ , where  $d_s^*$  is the sound horizon at decoupling (the distance a sound wave traveled from the big bang to the epoch of the CMB-baryons decoupling) and  $D_A^*$  is the angular diameter distance at decoupling, which in turn depends on the expansion history,  $H(z)$ , after decoupling, controlled also by the ratio  $\Omega_{DM}/\Omega_{DE}$  and  $H_0$  mainly. The  $w_0$ - $w_a$ CDM scenario is changing primarily the  $D_A^*$  history, because a faster expansion at late times increases the angular diameter distance to the surface of last scattering, thus generating high estimates on  $H_0$  parameter.

## 5 MODEL-INDEPENDENT RECONSTRUCTION OF THE DECELERATION PARAMETER

In this section, we will derive model-independent constraints on the deceleration parameter,  $q(z)$ , directly from analyses of the transversal BAO data. In order to do so, we use the so-called Gaussian Processes (GP) (Seikel et al. 2012; Rasmussen & Williams 2006). The GP has been shown to be a powerful tool to investigate cosmological parameter to some model-independent way (Arjona & Nesseris 2019; Shafieloo et al. 2012; Liao et al. 2020; Zhang & Li 2018; Wang & Meng 2017). In what follows, we briefly describe the methodology.

The GP method consists of considering Gaussian errors on data, so that the function that should describe the data correctly could be seen as a random normal variable. The method is explained in refs. Rasmussen & Williams (2006); Seikel et al. (2012); Jesus et al. (2020). As the data points are expected to be related through the same underlying function  $f(x)$ , two points  $x$  and  $x'$  are correlated through a covariance function (or kernel)  $k(x, x')$ . By choosing such a covariance function, the distribution of functions is described by

$$\begin{aligned} \mu(x) &= \langle f(x) \rangle, \\ k(x, x') &= \langle (f(x) - \mu(x))(f(x') - \mu(x')) \rangle, \\ \text{Var}(x) &= k(x, x). \end{aligned} \quad (4)$$

There are many choice options of the covariance functions, but without loss of generality, we shall focus on the Gaussian (or Squared Exponential) kernel, which is given by

$$k(x, x') = \sigma_f^2 \exp \left[ -\frac{(x - x')^2}{2l^2} \right], \quad (5)$$

where  $\sigma_f$  and  $l$  are the so called hyperparameters. The GP method consists on optimizing for  $\sigma_f$  and  $l$  and then using (4) for reconstruct the function  $f(x)$ .

We use the freely available software GaPP<sup>2</sup> in order to reconstruct  $q(z)$  from the  $\theta_{\text{BAO}}$  data. First, we have tried to reconstruct  $\theta_{\text{BAO}}(z)$ . However, we have found that the reconstruction of  $\theta_{\text{BAO}}(z)$  does not yield reliable results. As explained in Seikel et al. (2012), given the same amount of data, functions that change very rapidly are more difficult to reconstruct than smooth functions. It happens that  $\theta_{\text{BAO}}(z)$  is not a smooth function of the redshift  $z$ . In fact, for any cosmological model,  $D_A(z = 0) = 0$ . As  $\theta_{\text{BAO}}(z) \propto 1/D_A$ , then  $\theta_{\text{BAO}}(z) \rightarrow \infty$  for  $z \rightarrow 0$ .

Instead, we reconstruct  $D_A(z)$ , which is expected to be a smooth function of the redshift ( $D_A \propto z$  at low redshift for any cosmological model). In order to obtain the  $D_A(z)$  data, we have used Eq. (1) to obtain the uncertainties through error propagation as

$$\sigma_{D_A} = D_A \frac{\sigma_{\theta_{\text{BAO}}}}{\theta_{\text{BAO}}}. \quad (6)$$

The  $D_A(z)$  reconstruction can be seen on Figure 4. As observed in this figure (left panel), the reconstruction performs poorly in the range  $0.7 \lesssim z \lesssim 2$ , due to lack of data on this interval. Aiming to focus on the region with more available data, we perform a second reconstruction with BAO data only up to  $z < 0.7$ . This is shown in Figure 4 (right panel).

As can be seen in Figure 4 (right panel),  $D_A/r_{\text{drag}}$  is better constrained on  $0.4 < z < 0.7$ , where there is more data. For

<sup>2</sup> <http://www.acgc.uct.ac.za/~seikel/GAPP/index.html>

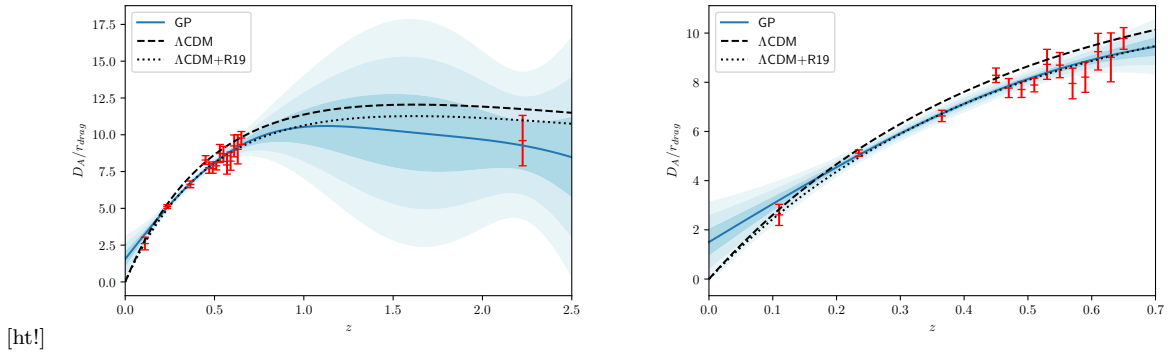


**Figure 4.** Reconstruction of  $D_A(z)/r_{\text{drag}}$ . The blue solid line corresponds to the median of  $D_A/r_{\text{drag}}$ . Also shown are the 68.3%, 95.4% and 99.7% CL regions. Left: Full sample. Right: Sample with  $z < 0.7$ .

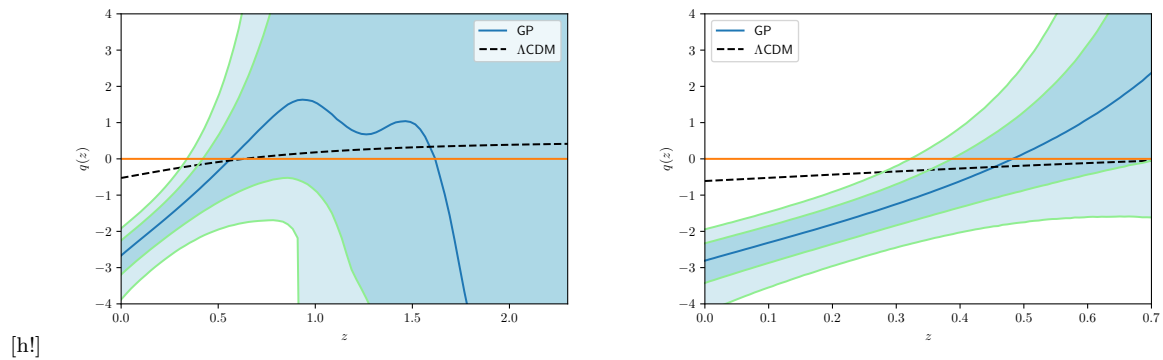


**Figure 5.** Reconstruction of  $q(z)$ . Also shown are the 68% and 95% CL regions. Left: Analyses of the full BAO data sample. Right: Analyses considering the sub-sample with  $z < 0.7$ .

$z < 0.4$ , there are only 3 data points, with a larger uncertainty for the lowest redshift datum. We believe this is the reason why the reconstruction poorly represents the expected behavior at low redshift, yielding a distance compatible with zero at  $z = 0$  only at the 99.7% CL.

Also observed in Figure 4, two predictions from  $\Lambda\text{CDM}$ , both using  $\Omega_m = 0.292$  and  $r_{\text{drag}} = 147.59$  Mpc, from the best fit of Planck+BAO combination. However, we have found that  $D_A$  is much sensitive to the choice of  $H_0$ . Thus, we show a curve with  $H_0 = 69.23$  km s $^{-1}$  Mpc $^{-1}$  from Planck + BAO (dashed curve) and one with  $H_0 = 74.03$  km s $^{-1}$  Mpc $^{-1}$  from R19 data (dotted curve). As can be seen the curve with higher value of the Hubble constant yields a better agreement with the data and with the GP reconstruction.

Assuming spatial flatness and the Etherington duality relation,  $D_L(z) = (1+z)^2 D_A(z)$ , and following the methodology given in ref. Jesus et al. (2020) (see section 3), we can write  $q(z)$  in the form

$$q(z) = -\frac{(1+z)^2 D_A''(z) + 3(1+z)D_A'(z) + D_A(z)}{D_A(z) + (1+z)D_A'(z)}. \quad (7)$$

From this result, the  $q(z)$  function is independent of the distance dimension, so it is independent of  $r_{\text{drag}}$ . We show the result of this reconstruction on Fig. 5. The blue solid line corresponds to the median  $q(z)$  obtained from the GP. The light blue regions correspond to the 68% and 95% CL around the median. These regions were found by sampling the

multivariate normal distribution of  $D_A$ ,  $D_A'$ , and  $D_A''$  found from the reconstruction above. We also show the theoretical prediction for  $\Lambda\text{CDM}$  (dashed curve) assuming  $\Omega_m = 0.292$  from Planck+BAO constraint. As can be seen, the  $\Lambda\text{CDM}$  model presents some tension with the reconstructed function done in light of the transversal BAO data only at low redshift,  $z < 0.3$ . This is probably due to the lack of data on this  $z$  range. On the other hand, in the interval  $0.3 < z < 0.7$ , with more data, there is a nice agreement with the  $\Lambda\text{CDM}$  cosmology using this model-independent reconstruction.

## 6 FINAL REMARKS

We have presented a new compilation with 15 angular BAO measurements summarized in Table 1 obtained from analyses of luminous red galaxies, blue galaxies, and quasars catalogs using various public data releases from the SDSS collaboration. As explained in the refs. Sánchez et al. (2011); Carnero et al. (2012); Carvalho et al. (2016), these transversal BAO data are weakly dependent on a cosmological model. It is worth mentioning that, due to the cosmological-independent methodology used to perform these transversal BAO measurements the errors calculated are larger than the errors obtained using a fiducial cosmology to model the BAO signal. The reason for this fact is that, while in the former methodology the error is given by the measure of how large is the BAO



bump, in the later approach the model-dependent best-fit of the BAO signal determines a smaller error. Typically, in the former methodology the error can be of the order of  $\sim 10\%$ , but in some cases it can arrive to 18%, instead, in the model-dependent approach it is of the order of few percent (Sánchez et al. 2011).

For the first time it is performed a combined analyses using these BAO data compilation, to explore the parameter space of some DE models and, additionally, obtain a precise estimate of  $r_{\text{drag}}$  from each model. Furthermore, we derive new bounds on the neutrino mass scale  $M_\nu$  within  $\Lambda$ CDM and extended models, considering the possibility for some dynamical DE scenarios. In addition, we perform an independent model analyses to reconstruct the deceleration parameter  $q(z)$  from the compilation of these BAO data.

An interesting outcome of the current analyses is that the addition of transversal BAO data helped to break possible degeneracy in the parameters space, showing the compatibility between Planck and these transversal BAO data sets. Last, but not least, we mention that the combination of the transversal BAO and CMB data can bound  $M_\nu$  with the same accuracy than other joint analyses reported in the literature. Finally, we observe that in the  $w_0 - w_a$ CDM model one can solve the current tension on the  $H_0$  parameter. Our results show that this current compilation with 15 BAO measurements, obtained free of any fiducial cosmology, can generate observational constrains compatible with other BAO compilations present in the literature. Therefore, it would be interesting to investigate these data in other cosmological contexts. For readers interested in using our BAO likelihood (python language), please contact us.

## ACKNOWLEDGEMENTS

The authors thank the referee for some clarifying points. RCN would like to thank the Brazilian Agency FAPESP for financial support under Project No. 2018/18036-5 and thanks the hospitality of Observatório Nacional, where part of this work was carried out. AB acknowledges a CNPq fellowship.

## DATA AVAILABILITY

The data underlying this article will be shared on request to the corresponding author.

## REFERENCES

- Abbott T. M. C. *et al.*, 2018, *Phys. Rev. D*, 98, 043526  
Ade P. A. R. *et al.* [Planck collaboration], 2011, *A&A* 536, A1  
Aghanim N. *et al.* [Planck collaboration], 2018a, preprint (arXiv:1807.06209)  
Aghanim N. *et al.* [Planck Collaboration], 2018b, preprint (arXiv:1807.06210)  
Aghanim N. *et al.* [Planck Collaboration], 2019, preprint (arXiv:1907.12875)  
Alcaniz J. S. *et al.*, 2017, *Fundam. Theor. Phys.*, 187, 11  
Anagnostopoulos F. K., Basilakos S., Saridakis E. N., 2019, *Phys. Rev. D*, 100, 083517  
Anselmi S., *et al.*, 2018, *Phys. Rev. Lett.*, 121, 021302  
Anselmi, S. *et al.*, 2019, *Phys. Rev. D*, 99, 123515  
Arjona R., Nesseris S., 2019, preprint (arXiv:1910.01529)  
Ata M. *et al.* [SDSS collaboration], 2018, *MNRAS*, 473, 4773  
Aubourg E. *et al.*, 2015, *Phys. Rev. D*, 92, 123516  
Audren B., Lesgourgues J., Benabed K., Prunet S., 2013, *JCAP*, 02, 001  
Bengaly C. A. P. *et al.*, 2017, *MNRAS*, 466, 2799  
Bernal J. L., Verde L., Riess A. G., 2016, *JCAP*, 10, 019  
Bernui A., Tsallis C., Vilella T., 2006, *Physics Letters A*, 356, 426  
Bernui A., Tsallis C., Vilella T., 2007, *Europhysics Letters*, 78, 19001  
Bernui A., Ferreira I. S., Wuensche C. A., 2008, *Astrophys. J.*, 673, 968  
Blas D., Lesgourgues J., Tram T., 2011, *JCAP*, 07, 034  
Camarena D., Marra V., 2019, preprint (arXiv:1910.14125)  
Capozziello S., D’Agostino R., Luongo O., 2019, *Int. J. Mod. Phys. D*, 28 10, 1930016  
Carnero A., Sanchez E., Croce M., Cabre A., Gaztanaga E., 2012, *MNRAS*, 419, 1689  
Carter P., Beutler F., Percival W. J., DeRose J., Wechsler R. H., Zhao C., 2020, to appear in *MNRAS*, preprint (arXiv:1906.03035)  
Carvalho, G. C., Bernui, A., Benetti, M., Carvalho, J. C., Alcaniz, J. S., 2016, *Phys. Rev. D*, 93, 023530  
Carvalho, G. C., Bernui, A., Benetti, M., Carvalho, J. C., de Carvalho, E., Alcaniz, J. S., 2020, *Astropart. Phys.*, 119, 102432  
Chevallier M., Polarski D., 2001, *Int. J. Mod. Phys. D*, 10, 213  
Choudhury S. R., Choubey S., 2018, *JCAP*, 09, 017  
D’Agostino R., Nunes R. C., 2019, *Phys. Rev. D*, 100, 044041  
de Carvalho E., Bernui A., Carvalho G. C., Novaes C. P., Xavier H. S., 2018, *JCAP*, 04, 064  
de Carvalho E., Bernui A., Xavier H. S., Novaes C. P., 2020, *MNRAS*, 492, 4469  
de Carvalho E. *et al.*, 2020, submitted to *ApJ*  
Di Valentino E., Melchiorri A., Silk J., 2019a, *Nat. Astron.*, 4, 2  
Di Valentino E., Melchiorri A., Silk J., 2019b, preprint (arXiv:1908.01391)  
Di Valentino E., Melchiorri A., Mena O., Vagnozzi S., 2020a, *Phys. Rev. D*, 101, 063502  
Di Valentino E., Melchiorri A., Silk J., 2020b, preprint (arXiv:2003.04935)  
Eisenstein D. J. *et al.* [SDSS Collaboration], 2005, *Astrophys. J.*, 633, 560  
Giusarma E., Gerbino M., Mena O., Vagnozzi S., Ho S., Freese K., 2016, *Phys. Rev. D*, 94, 083522  
Haridasu B. S., Luković V. V., D’Agostino R., Vittorio N., 2017, *A&A* 600, L1  
Heavens A., Jiménez R., Verde L., 2014, *Phys. Rev. Lett.*, 113, 241302  
Hinshaw G. *et al.* [WMAP collaboration], 2013, *Astrophys. J. Suppl.*, 208, 19  
Ishak M., 2019, *Living Reviews in Relativity*, 22, 1  
J. F. Jesus, R. Valentim, A. A. Escobal and S. H. Pereira, 2020, *JCAP* 04 053  
Kumar S., Nunes R. C., Yadav S. K., 2018, *Phys. Rev. D*, 98, 043521  
Kumar S., Nunes R. C., Yadav S. K., 2019, *Eur. Phys. J. C*, 79, 576  
Lattanzi M., Gerbino M., 2018, *Front. in Phys.*, 5, 70  
Lesgourgues J., Pastor S., 2006, *Phys. Rept.*, 429, 307  
Liao K., Shafieloo A., Keeley R. E., Linder E. V., 2020, preprint (arXiv:2002.10605)  
Linder E. V., 2003, *Phys. Rev. Lett.*, 90, 091301  
Lindner M., Max K., Platscher M., Rezacek J., 2020, preprint (arXiv:2002.01487)  
Loureiro A. *et al.*, 2019, *MNRAS*, 485, 326  
Marques G. A., Novaes C. P., Bernui A., Ferreira I. S., 2018, *MNRAS*, 473, 165  
Marques G. A., Liu J., Matilla J. M. Z., Haiman Z., Bernui A., Novaes C. P., 2019, *JCAP*, 06, 019

- Marra V., Isidro E. G. C., 2019, *MNRAS*, 487, 3419
- Nesseris S., Sapone D., Sypsas S., 2019, *Phys. Dark Univ.*, 27, 100413
- Novaes C. P., Bernui A., Ferreira I. S., Wuensche C. A., 2014, *JCAP*, 01, 018
- Novaes C. P., Bernui A., Ferreira I. S., Wuensche C. A., 2015, *JCAP*, 09, 064
- Nunes R. C., Pan S., Saridakis E. N., Abreu E. M. C., 2017, *JCAP*, 01, 005
- Nunes R. C., 2018a, *JCAP*, 05, 052
- Nunes R. C., Bonilla A., 2018b, *MNRAS*, 473, 4404
- O'Dwyer M., Anselmi S., Starkman G. D., Corasaniti P., Sheth R. K., Zehavi I., 2019, preprint (arXiv:1910.10698)
- Pan S., Yang W., Di Valentino E., Shafieloo A., Chakraborty S., 2019a, preprint (arXiv:1907.12551)
- Pan S., Yang W., Di Valentino E., Saridakis E. N., Chakraborty S., 2019b, preprint (arXiv:1907.07540)
- Poulin V., Smith T. L., Karwal T., Kamionkowski M., 2019, *Phys. Rev. Lett.*, 122, 221301
- Riess A. G. *et al.*, 2019, *Astrophys. J.*, 876, 85
- Salazar-Albornoz S. *et al.*, 2017, *MNRAS*, 468, 2938
- Sánchez E. *et al.*, 2011, *MNRAS*, 411, 277
- Seikel M., Clarkson C., Smith M., 2012, *JCAP*, 06, 036
- Shanks T., Hogarth L. M., Metcalfe N., 2019, *MNRAS Lett.*, 484, L64
- Sutherland W., 2012, *MNRAS*, 426, 1280
- Rasmussen C., Williams C., 2006, *Gaussian Processes for Machine Learning*, MIT Press, Cambridge, U.S.A.
- Shadab A. *et al.* [SDSS collaboration], 2017, *MNRAS*, 470, 2617
- Shafieloo A., Kim A. G., Linder E. V., 2012, *Phys. Rev. D*, 85, 123530
- Suzuki N. *et al.* [The Supernova Cosmology Project], 2012, *Astrophys. J.*, 746, 85
- Vagnozzi S., Giusarma E., Mena O., Freese K., Gerbino M., Ho S., Lattanzi M., 2017, *Phys. Rev. D*, 96, 123503
- Vagnozzi S., Dhawan S., Gerbino M., Freese K., Goobar A., Mena O., 2018, *Phys. Rev. D*, 98, 083501
- Vagnozzi S., 2019, preprint (arXiv:1907.07569)
- Vagnozzi S., Visinelli L., Mena O., Mota D. F., 2020, *MNRAS*, 493, 1139
- Vargas-Magaña M. *et al.*, 2018, *MNRAS*, 477, 1153
- Weinberg D. H., Mortonson M. J., Eisenstein D. J., Hirata C., Riess A. G., Rozo E., 2013, *Phys. Rept.*, 530, 87
- Yang W., Di Valentino E., Mena O., Pan S., Nunes R. C., 2020, preprint (arXiv:2001.10852)
- Yang W., Nunes R. C., Pan S., Mota D. F., 2017, *Phys. Rev. D*, 95, 103522
- Yang W., Pan S., Di Valentino E., Nunes R. C., Vagnozzi S., Mota D. F., 2018, *JCAP*, 09, 019
- York D. G. *et al.* [SDSS Collaboration], 2000, *Astrophys. J.*, 120, 1579
- Wang D., Meng X. H., 2017, *Phys. Rev. D*, 95, 023508
- Zhang M. J., Li H., 2018, *Eur. Phys. J. C*, 78, 460